Int. J. Electrochem. Sci., 7 **(2012)** 10175 - 10189

International Journal of
ELECTROCHEMICAL
SCIENCE
www.electrochemsci.org

Synthesis and Characterization of Electrochemically Platinum-Polyaniline Modified Carbon Textile Electrodes

Javier Fernández, Javier Molina, Ana I. del Río, José Bonastre, Francisco Cases[*]

Departamento de Ingeniería Textil y Papelera, Escuela Politécnica Superior de Alcoy, Universitat Politècnica de València. Plaza Ferrándiz y Carbonell, s/n, 03801, Alcoy, Spain.
[*]E-mail: fjcases@txp.upv.es

Received: 18 August 2012 / *Accepted:* 13 September 2012 / *Published:* 1 October 2012

The present work deals with the use of a carbon fiber fabric for electrochemical purposes. To carry out such investigation, suitable working electrodes of C, Pt/C and Pt/PANI/C were manufactured. Two types of electrodes were made from: Yarns pulled out from the woven textile (CYEs) and strips, 1 cm x 2 cm area, cut from the fabric (CSEs). Cyclic voltammetry (CV) was employed to carry out the electrosynthesis processes. Cyclic and linear voltammetry, electrochemical impedance spectroscopy (EIS) and scanning electrochemical microscopy (SECM) were used to study the electrocatalytic properties of carbon modified electrodes (CMEs). X-ray photoelectron spectroscopy (XPS) and scanning electron microscopy (SEM) were used to know the chemical composition and to describe the morphology of the Pt/PANI/C and Pt/C modified surfaces. Sulphuric and amaranth solutions were chosen for the electrochemical experiments considering the possible applications of CMEs in the field of electrochemical treatment of industrial wastewater polluted with azo dyes.

Keywords: Textile carbon electrode; Polyaniline; Platinum electrodeposition; Amaranth.

1. INTRODUCTION

The use of textiles as material for electrodes provides great versatility. In this sense, it is possible to act on the geometry of the electrodes and consequently on the design of electrochemical cells. Moreover, textiles are materials relatively cheap and simple to manufacture. On the other hand, an activated carbon fiber presents electric conductivity. This property provides the advantage of the direct modification of the textile surface by means of electrochemical procedures. Non conductive textiles require a previous chemical transformation in order to gain conductivity [1-2]. The experimental conditions of an electrochemical process are easier to control than the chemicals ones.

Textile dyeing and finishing wastewaters are usually polluted with non-fixed dyes. Dyes are chemicals that even at low concentrations induce a high color in effluents. In addition, many of these dyes may be toxic and/or mutagenic to aquatic life [3]. Taking into account that dyes present difficulties to biological degradation, electrochemical treatment would be an attractive option for textile wastewater treatment. Therefore, over the past 10 years, the electrochemical techniques have been found of special interest for textile wastewater treatment due to advantages such as high efficiency, ease of operation and environmental compatibility since there is no need of adding chemicals [4]. In the light of the above, several works have focused on the destruction of these synthetic wastes using electrochemical oxidation [5-10], although electrochemical reduction has been also found as an interesting method for a suitable decolorization of textile wastewaters [11-14]. Fan et al. [15] studied the electrochemical degradation, under galvanostatic conditions, of amaranth aqueous solution onto an activated carbon fiber (ACF) electrode. ACF is described as a comparatively modern form of porous carbon material over the traditional powder or granular forms. Kezhong et al. [16] studied the catalytic activity of platinum-polyaniline modified carbon fiber electrodes for the electrooxidation of methanol.

The aim of the present research was to improve the catalytic properties of an activated carbon fabric by electrodepositing Pt directly onto bare carbon and onto polyaniline modified carbon surfaces. In this sense, Pt/C and Pt/PANI/C electrodes were examined in sulphuric and amaranth/sulphuric media in order to establish their electrochemical behavior. The electrochemical treatment of azo dyes used in textile industry is a matter of special interest since it is one of the main study lines of our research group. Cyclic voltammetry (CV), linear voltammetry (LV), electrochemical impedance spectroscopy (EIS), and scanning electrochemical microscopy (SECM) were the techniques used to carry out the electrochemical studies.

X-ray photoelectron spectroscopy (XPS) was used to study the chemical composition of the modified surfaces and the doping ratio of PANI. Scanning electron microscopy (SEM) was employed to study the morphology of the different surfaces.

2. MATERIALS AND METHODS

2.1. Working electrode preparation

The company Carbongen S.A., Cocentaina, Spain, supplied an activated carbon fabric with hydrophilic properties. In order to rule out the presence of impurities on the surface of the fabric, a previous analysis by infrared spectroscopy (FTIR-ATR) was carried out. Technical characteristics of the activated carbon fabric are presented in Table 1. An image of the woven textile is shown in Figure 1. The yarns are not tightly woven, weft and warp leave empty spaces and some filaments are loose. The inset shows a SEM micrograph of the carbon filaments.

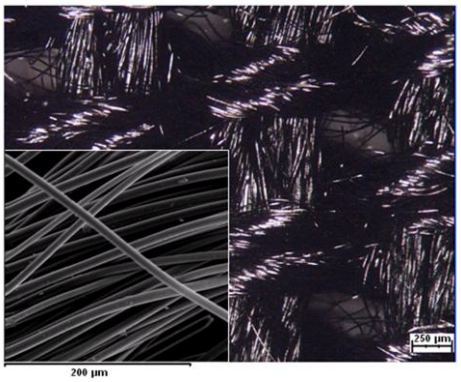

Figure 1. Image of the carbon woven textile. The inset shows a SEM micrograph of the carbon fibers.

With the purpose of preparing suitable working electrodes, two types of electrodes were tested. The first type was prepared from 5 mm yarns pulled out from the woven textile. The second one was made from strips 1 cm x 2 cm area cut from the fabric. In order to ensure a proper electric contact, carbon samples and a copper wire (diameter 250 µm) were glued with CircuitWorks® Conductive Epoxy by Chemtronics®. The solder was hardened in an oven at 100 ºC.

Table 1. Parameters of the activated carbon fabric used in the present investigation.

Parameters	Units	Values
Weight	g/m^2	105 ± 5
BET[a]	m^2/g	1100 ± 100
Iodine index[b]	mg I_2/g	1100 ± 50
Permeability[c]	mm/s	728 ± 44
Thickness[d]	mm	0.505 ± 0.016
Tensile strength[e]. Warp	N	230 ± 23
Tensile strength[e]. Weft	N	120 ± 18
Elongation[e]. Warp	%	4.60 ± 1.19
Elongation[e]. Weft	%	8.28 ± 0.40
LOI[f]	%	48

(a) BET: Brunauer, Emmet and Teller. Results got applying this statistical equation to N_2 isotherm adsorption at -196 ºC.
(b) ASTM D 4607-86 modified using photometric determination.
(c) UNE EN ISO 9237:1996.
(d) UNE EN ISO 5084:1997.
(e) UNE EN ISO 13934-1:1999.
(f) UNE EN ISO 4589-2:2001.

2.2. Experimental facility and materials

Two experimental set-ups were prepared. A conventional voltammetric cell was employed for the experiments with the CMYEs. Two rods of stainless steel (3.5 cm diameter) were used as counter electrodes. For the CMEs a 250 cc beaker was used as a vessel. The counter electrode was a stainless steel cylindrical mesh (height: 4.5 cm, diameter: 3.5 cm). The textile electrode was placed in the middle of the cylinder and immersed 1 cm to prevent that the solution reaches the solder by capillarity. For both set-ups all the potential measurements were referred to Ag/AgCl (3 M KCl) reference electrode.

The voltammetric experiments were performed with an Autolab PGSTAT302 potentiostat/galvanostat. The ohmic potential drop (Ω) was measured and introduced in the Autolab software (GPES).

EIS experiments were also performed with the Autolab PGSTAT302 potentiostat/galvanostat in the 10^4–10^{-2} Hz frequency range. The amplitude of the sinusoidal voltage employed was ±10 mV. Each measurement was carried out at a constant imposed potential equal to the stabilized open circuit potential (OCP) at the beginning of the experiment. A standard three-electrode design was employed. The electrolyte resistance data was obtained replacing the working electrode by a Pt one. To analyze quantitatively the electrochemical behavior of the samples, the experimental impedance data were modeled and fitted to data generated by using suitable electrical equivalent circuits and a non-linear least squares fitting minimization method included in the ZPlot/ZView software (3.1c version) from Scribner Associates Inc, Southern Pines, NC, USA.

SECM measurements were carried out with a scanning electrochemical microscope of Sensolytics. The three-electrode cell configuration consisted of a Pt ultramicroelectrode (UME) working electrode, a Pt wire as auxiliary electrode and an Ag/AgCl (3 M KCl) as reference electrode. UMEs of 10 and 100 μm diameter were used in the present work. The SECM experiments were carried out in a 0.01 M $Ru(NH_3)_6Cl_3$ and 0.1 M K_2SO_4 solution. The pH was adjusted with 0.01 M KOH and 0.01 M H_2SO_4 solutions. Strip samples of Pt/PANI/C and PANI/C were treated during 1 hour at pH 2.5 or 9.0. Once dried in a desiccator, samples of 5 mm x 5 mm were cut and glued with epoxy resin on glass microscope slides. SECM experiments were performed at OCP that is to say; the potential of the substrate is indirectly controlled by the redox couple concentration.

Oxygen was removed from solutions in all electrochemical experiments by bubbling nitrogen gas (N_2 Premier X50S) and then a N_2 atmosphere was maintained. The solutions were prepared with ultrapure water obtained from an Elix 3 Millipore-Milli-Q Advantage A10 system with a resistivity near to 18.2 MΩ·cm. Aniline was purified by distillation before use. All the reagents were analytical grade and used as received. The amaranth solutions were prepared from the commercial product.

XPS analyses were conducted at a base pressure of $5x10^{-10}$ mbars and a temperature around -100 ºC. XPS spectra were obtained with a VG-Microtech Multilab electron spectrometer by using unmonochromatized Mg Kα (1253.6 eV) radiation from a twin anode source operating at 300 W (20 mA, 15 kV). The binding energy (BE) scale was calibrated with reference to the C1s line at 284.6 eV. N1s and Pt4f core levels XPS spectra were analyzed for the different samples.

A Jeol JSM-6300 scanning electron microscope was employed to observe the morphology of the samples. SEM analyses were performed using an acceleration voltage of 20 KV. Previously to their observation the samples were coated with gold employing a sputter Bal-Tec SCD 005. The samples analyzed by SEM come from the CMY electrodes cut by the solder point to prevent the deterioration of the yarn.

3. RESULTS AND DISCUSSION

3.1. Research using CYEs

3.1.1. PANI synthesis by cyclic voltammetry.

A CYE was introduced in a 0.1 M freshly distilled aniline and 0.5 M H_2SO_4 aqueous solution. The electropolymerization of aniline was carried out by cycling the potential between -125 mV and 875 mV for several cycles at 20 $mV \cdot s^{-1}$. Figure 2a shows the CVs recorded during the electropolymerization process. It can be clearly seen the increase of the intensity of the different electrochemical processes with the number of scan. This indicates that the synthesis of polyaniline is taking place. Figure 2b shows the cyclic voltammogram of a modified yarn electrode after ten electropolymerization cycles in 0.5 M H_2SO_4.

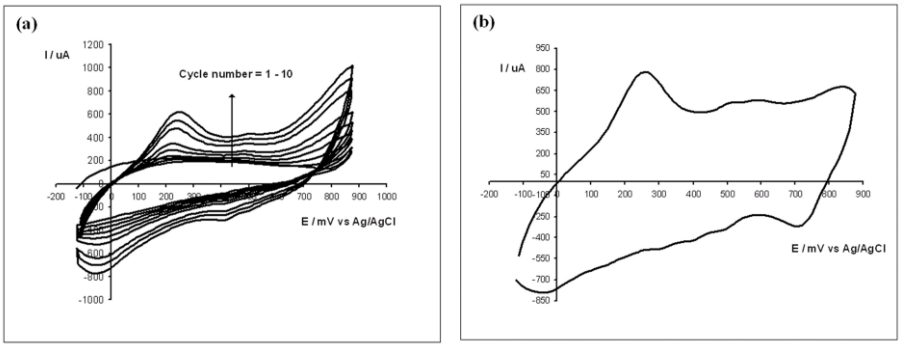

Figure 2. (a) Cyclic voltammograms recorded during electropolymerization of aniline on a carbon electrode in aniline 0.1 M and 0.5 M H_2SO_4 solution. Scan rate 20 $mV \cdot s^{-1}$. (b) Cyclic voltammogram of a PANI/C electrode (synthesized after ten polymerization cycles) in 0.5 M H_2SO_4 solution. Scan rate 20 $mV \cdot s^{-1}$.

Characteristic peaks at around 250 mV, 600 mV and 850 mV, respectively assigned for the conversion of leucoemeraldine to emeraldine, redox reaction of degradation products (hydroquinone to quinone) and emeraldine to pernigraniline, are clearly identified [17]. Based on these results, ten electropolymerization cycles are considered adequate to get a useful PANI/C electrode. In order to describe the morphology of the polymer on PANI/C electrode, a SEM micrograph was recorded in the micrometer range. According to Figure 3, the potentiodinamic method used to synthesize the polymer produces PANI with fibrous structure.

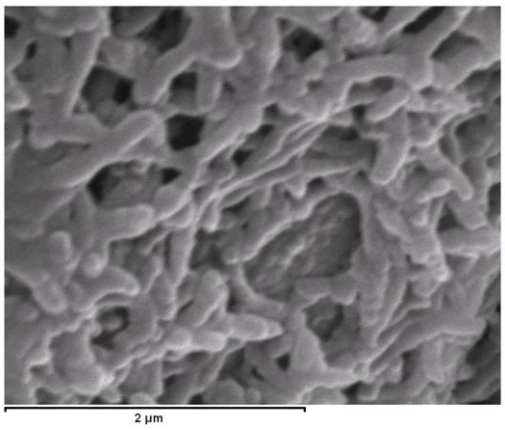

Figure 3. SEM micrograph of the electropolymerized polyaniline structure recorded at 25000x magnification.

3.1.2. Cyclic voltammetry of Pt electrodeposition.

Cyclic potential method was chosen for the electrodeposition of platinum since it provides a proper catalytic activity compared to other procedures such as constant potential or double potential step [18]. Platinum electrodeposition was performed onto both electrodes (bare carbon textile electrode and polyaniline modified carbon textile electrode) in 5 mM $H_2PtCl_6.6H_2O$ and 0.5 M H_2SO_4 solution by cycling the potential between -250 mV and 400 mV at 10 $mV \cdot s^{-1}$. Figure 4 shows the CVs obtained during the electrodeposition process on C and PANI/C electrodes.

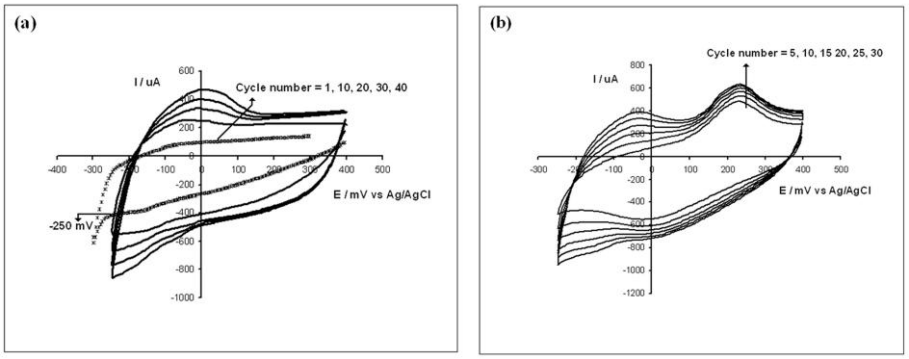

Figure 4. (a) Cyclic voltammograms obtained during electrodeposition of platinum (1st, 10th, 20th, 30th, 40th cycles) on bare carbon electrode. (b) Cyclic voltammograms obtained during electrodeposition of platinum (5th, 10th, 15th, 20th, 25th, 30th cycles) on polyaniline modified carbon electrode. Both voltammograms were recorded in a 5 mM H_2PtCl_6 and 0.5 M H_2SO_4 solution. Scan rate 10 $mV \cdot s^{-1}$.

In order to establish the reduction potential limit, a CYE was previously cycled between -300 mV and 400 mV (1st cycle of Figure 4a). Thus a potential of -250 mV was selected as reduction

potential limit. An increment of the current was observed in the CVs from Figure 4a and Figure 4b as the number of electrodeposition cycles increased.

3.1.3. Pt/C and Pt/PANI/C electrochemical characterization in sulphuric acid solution

Different Pt/C and Pt/PANI/C electrodes were characterized by CV in 0.5 M H_2SO_4. The CVs recorded are shown in Figure 5. As it is shown in Figure 5a, only the platinum modified carbon electrodes obtained with the 20th, 30th and 40th platinum electrodeposition cycles exhibit the characteristic oxidation and reduction peaks of a bulk Pt electrode in sulphuric medium [19]. Figure 5b shows the CVs recorded for Pt/PANI/C (after the 20th and 30th platinum electrodeposition cycles) electrodes. As it can be seen, only the peak due to the transformation of PANI from leucoemerandine to emeraldine is visible.

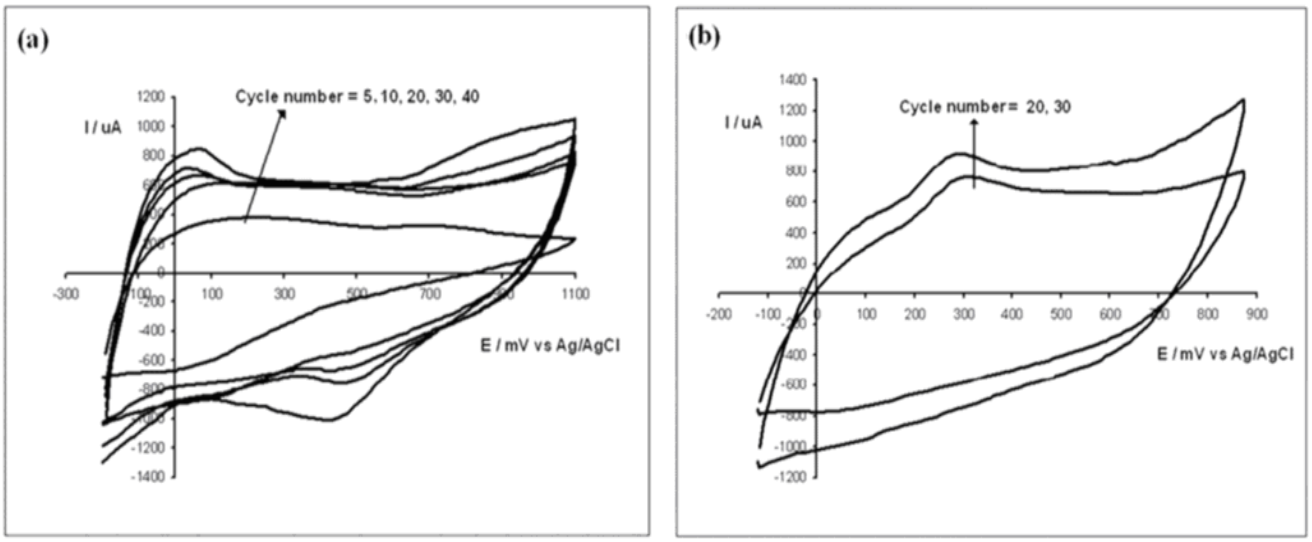

Figure 5. (a) Cyclic voltammograms of Pt/C (5th, 10th, 20th, 30th, 40th deposition cycles) in 0.5 M H_2SO_4 solution. Scan rate 20 mV·s^{-1}. (b) Cyclic voltammograms of Pt/PANI/C (20th, 30th deposition cycles) in 0.5 M H_2SO_4 solution. Scan rate 20 mV·s^{-1}

3.1.4. Amaranth electrochemical behavior on bare C, Pt/C and Pt/PANI/C

The amaranth polarization curves were obtained for bare C, Pt/C and Pt/PANI/C electrodes (Pt/C and Pt/PANI/C were obtained after the 25th platinum electrodeposition cycle) in 1mM amaranth and 0.5 M H_2SO_4 solution. Figure 6 shows the polarization curves obtained in the potential range from -200 to 900 mV (the reduction potential -200 mV was maintained for 200 s). No characteristic peak was observed on bare C electrode. On the contrary, Pt/C and Pt/PANI/C polarization curves show a typical peak at around 460 mV. When the potential range started at 250 mV no peak was observed.

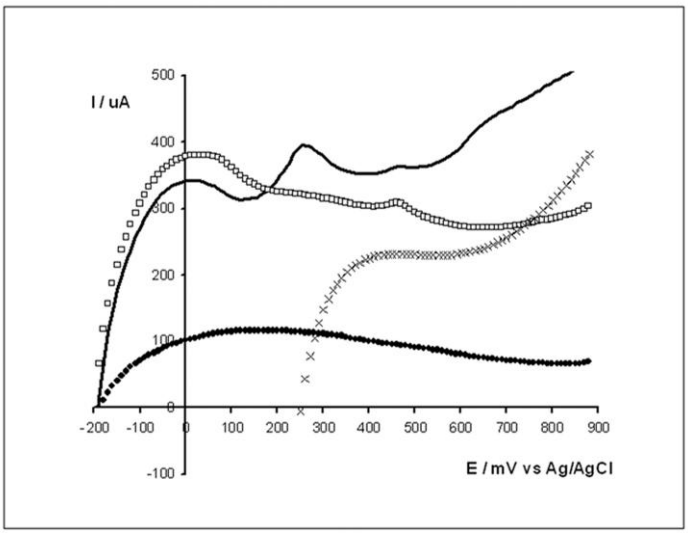

Figure 6. Polarization curves obtained for bare C (**…**), Pt/C (□), Pt/PANI/C (□) electrodes (25th deposition cycles), starting potential -200 mV, and Pt/C (xxx) starting potential 250 mV. Scan rate 10 mV·s^{-1}. The polarization curves were obtained in 1 mM amaranth and 0.5 M H_2SO_4 solution.

A plausible explanation for this result could be given by the fact that at -200 mV a first degradation of the amaranth molecule would have happened. Then an intermediate product from the electroreduction would be electrooxidized giving an oxidation peak at 460 mV. This voltammetric behavior of Pt/C and Pt/PANI/C in the presence of amaranth dye was also observed in voltammetric experiments focused on characterization of azo dyes using Pt and dispersed Pt/PANI/Pt electrodes [20].

3.1.5. EIS study in sulphuric solution

The electrical properties of C, Pt/C, PANI/C and Pt/PANI/C electrodes were tested in a 0.5 M sulphuric solution to measure its electrical changes. For these conductive materials in solution it can be expected the following contributions to its impedance:

- R_e: Electrolyte resistance + electronic resistance of the conductive material (R_{film}).

- R_{ifs}: Ionic charge transfer resistance at the conductive material/solution interface corresponding to the counter-ion exchange.

- C_{ifs}: Space charge capacitance at the conductive material/solution interface corresponding to the counterion exchange.

- W: Warburg impedance due to counter-ion diffusion. W-R: Diffusion resistance. W-T: l^2/D (s), l: length of the diffusion layer, D: binary electron–ion diffusion coefficient. W-P: Warburg exponent.

The Nyquist plots for the different electrodes are shown in Figure 7.

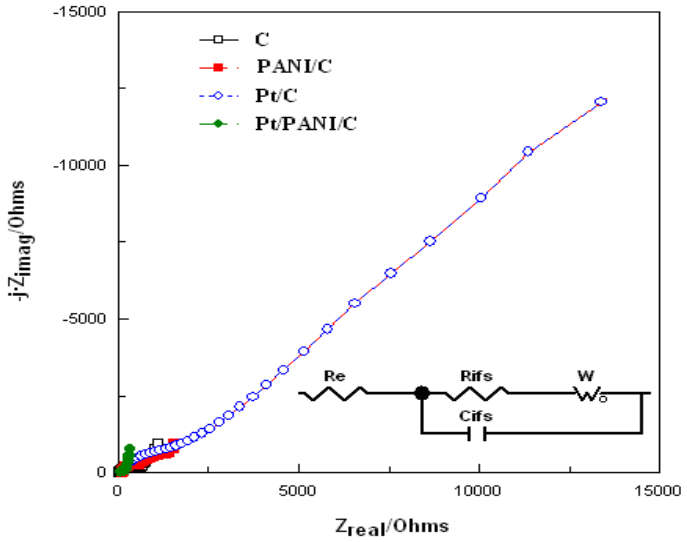

Figure 7. Nyquist plots of conductive materials immersed in 0.5M H_2SO_4. Frequency range from 10^4 to 10^{-2} Hz. The inset shows the proposed equivalent circuit.

Experimental data were fitted with the equivalent circuit proposed in the inset and the different parameters obtained are shown in Table 2. According to Figure 7 high impedance values for Pt/C electrode were obtained. Diffusion in this electrode is hindered. Nyquist plots also show the low impedance values for Pt/PANI/C electrode. Seeing Table 2, it can be said that values for Warburg impedance were lower for Pt/PANI/C electrode. In addition, the ionic charge transfer resistance (R_{ifs}) is at least four times lower than that for the other electrodes. The capacitance (C_{ifs}) was very high for both PANI electrodes due to their supercapacitor properties [21].

The fitting data in Table 2 show that the electronic resistance of the films is lower for the carbon textile electrode and for P/PANI/C electrode (best conductivity) in comparison with the other electrodes. Taking into account these results, the electroactivity has been increased significantly for the Pt/PANI/C electrode.

Table 2. Results of the fitting of impedance data of conductive materials in 0.5M H_2SO_4. Resistance units in Ω and capacitance units in F.

Conductive fabrics	C	PANI/C	Pt/C	Pt/PANI/C
$R_{Electrolyte}$	5	5	5	5
R_{film}	81	123	172	75
R_{ifs}	218	233	711	55
C_{ifs}	$8x10^{-6}$	$140x10^{-6}$	$2x10^{-6}$	$400x10^{-6}$
W-R	850	3953	98700	244
W-T	11	168	604	4
W-P	0.3	0.4	0.4	0.4

3.2. SECM study for using the CMS electrodes.

No proper voltammetric information could be obtained with CMSEs; so the parameters of synthesis established for (CMYEs) were used in the voltammetric synthesis of (CMSEs). According to this information the potential range was established between [-125, 1100] mV for the electropolymerization process and [-250, 400 mV] for the electrodeposition of platinum. The scan rate employed was 5 $mV \cdot s^{-1}$.

SECM technique has been proved as a very useful technique to show the electrochemical properties of these textile substrates. Samples of Pt/C, PANI/C and Pt/PANI/C were prepared with ten electropolymerization cycles of aniline and twelve electrodeposition cycles of Pt. Approach (I_T–L) curves were recorded in the feedback mode with the Pt tip held at a potential of -350 mV. This potential was kept constant in order to reduce the oxidized form of the mediator, $Ru(NH_3)_6^{3+}$, at a diffusion controlled rate. These approach curves give an indication of the electroactivity of the electrode surface. If the surface is non conductive, when the UME approaches the surface there is a decrease of the normalised current (I_T) (negative feedback). On the other hand if the substrate is conductive, when the UME approaches the surface the normalised current (I_T) increases (positive feedback) [22]. The normalized current, I_T, is defined as $I_T = i/id_{inf}$ where $id_{inf} = 4nFaDC_{bulk}$ is the steady diffusion current, n is the number of electrons, F is the Faraday constant, a is the radius of the UME, D is the diffusion coefficient and C_{bulk} is the bulk concentration of the mediator. Figure 8 shows a selection of the experimental curves recorded at pH 2.5 or 9.0. The approaching curve for the theoretical positive feedback model has been also included for comparison.

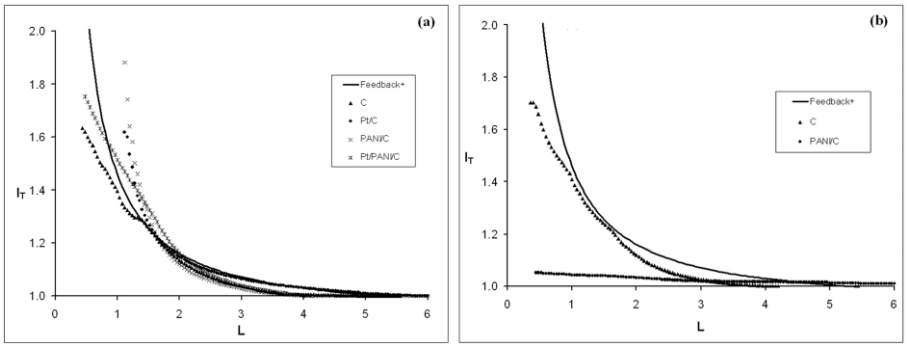

Figure 8. (a) Approach curves on unbiased (OCP = 0.5 V) C, Pt/C, PANI/C and Pt/PANI/C at (a) pH = 2.5. (b) Approach curves on unbiased (OCP = 0.5 V) C and PANI/C at pH = 9.0. The approach curves were recorded with a Pt UME tip (diameter 100 μm) in 0.01M $Ru(NH_3)_6$ and 0.1M K_2SO_4 solution. The tip potential was -350 mV (vs Ag/AgCl) and the approach rate was 25 $mV \cdot s^{-1}$.

The theoretical curve has been obtained taking into account the RG value of the UMEs. The RG value is defined as RG = Rg/a, where Rg is the radius of the insulating glass surrounding the tip of radius a. The RG of our UME tip is RG ≥ 20. Pade's approximation [23] gives an approximate and simple equation with low relative error for all distances and valid for RG > 10. The approximate

expression of the steady-state normalized current assuming positive feedback for a UME with finite insulator thickness is:

$$I_T{}^C = \frac{1+\frac{1.5647}{L}+\frac{1.316855}{L^2}+\frac{0.4919707}{L^3}}{1+\frac{1.1234}{L}+\frac{0.626395}{L^2}}$$

where L is the normalized distance defined as L = d/a (d is the UME–substrate separation and a is the UME radius). Figure 8a shows the approach curves recorded on unbiased (OCP = 0.5 V) C, PANI/C, Pt/C and Pt/PANI/C at pH = 2.5. All of them show a conductive behavior. This result indicates that the carbon fiber employed in the woven textile is a good conductive support for modified electrodes.

On the other hand, Figure 8b shows the approach curve on a deactivated PANI/C sample. Taking into account the conductivity of the bare carbon sample at pH = 9.0, the loss of conductivity of PANI/C is an evidence of the proper distribution of the polymer on the surface. To distinguish the distribution of the disperse Pt on the surface of PANI/C, a sample of Pt/PANI/C was studied at pH = 9.0.

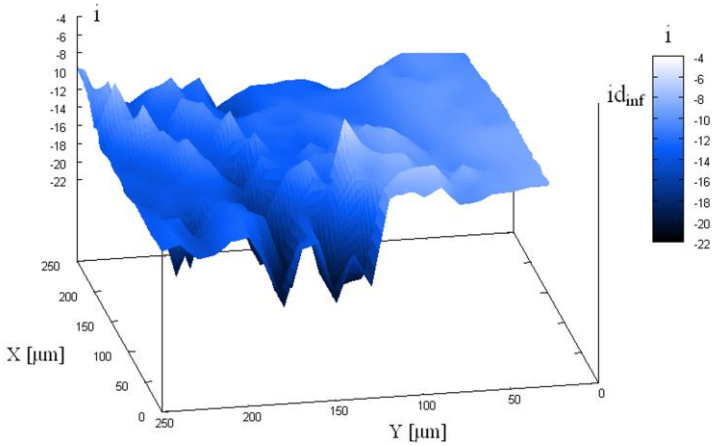

Figure 9. 3D SECM image of the electrochemical activity of an unbiased (OCP = 0.5 V) Pt/PANI/C surface at pH = 9.0. The image was recorded with a Pt UME tip (diameter 10 µm) in 0.01 M $Ru(NH_3)_6$ and 0.1 M K_2SO_4 solution. The tip potential was -350 mV (vs Ag/AgCl) and the scanning rate was 20 $\mu m \cdot s^{-1}$ with step increments of $\Delta x = \Delta y = 10$ µm. Bulk current id_{inf} = 8.0 nA.

Figure 9 shows a 3D image of the electrochemical activity. The arrayscan, recorded at constant height mode, shows areas of positive feedback ($i > id_{inf}$ = 8.0 nA) corresponding to high concentration of Pt particles and certain moieties of negative feedback ($i < id_{inf}$ = 8.0 nA) corresponding to the deactivated PANI. The conductive areas (positive feedback) on the modified surface are predominant. Both topography and conductive nature of the substrate appear in the 3D SECM image. At constant

height experiment, the distance between UME tip and substrate varies during the X-Y scanning, so the different degrees of feedback in SECM image are due to the contributions of electrochemical activity and topography.

3.3. Scanning electron microscopy (SEM) and X-ray photoelectron spectroscopy (XPS)

In this section modified CYEs have been studied. Figure 10 displays the morphology of Pt/C and Pt/PANI/C (obtained in both cases after the 25th platinum electrodeposition cycle) electrodes taken at a magnification of 3000x. The Figure 10a shows a compact distribution of platinum particles for Pt/C electrode. On the other hand, the surface of Pt/PANI/C electrode (Figure 10b) shows a lower number of platinum particles and a more disperse distribution of the platinum.

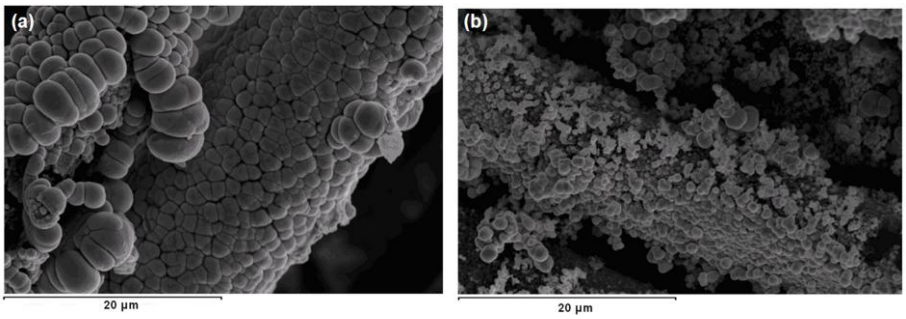

Figure 10. SEM micrograph (a) of Pt/C (25th cycle) surface and (b) Pt/PANI/C (25th cycle) surface. Both micrographs were taken at 3000x magnification

X-ray photoelectron spectroscopy (XPS) measurements were performed to determine the chemical states as well as the relative Pt content in the coatings. Samples of Pt/C and Pt/PANI/C obtained after the 25th platinum electrodeposition cycle were analyzed. The high resolution Pt4f spectrum for the Pt/PANI/C sample is shown in Figure 11a. The relative Pt content in the Pt/PANI/C sample (% atomic) was 11.81 %. Four deconvoluted peaks appeared in this spectrum. The two peaks at 71.2 eV ($Pt4f_{7/2}$) and 74.4 eV ($Pt4f_{5/2}$) were attributed to a spin-orbit coupling doublet. The doublet separation of 3.2 eV is characteristic for the platinum element (Pt4f) [24, 25]. These binding energies were due to metallic Pt [25-27]. Other doublet was observed at 72.8 and 76.0 eV. This doublet was assigned to Pt^{2+} species [28-29] such as PtO or $Pt(OH)_2$. About 26 % of the total Pt content was in the Pt^{2+} form; it was not completely reduced to metallic Pt by the electrodeposition method.

Figure 11b shows the high resolution Pt4f spectrum for the Pt/C sample. The relative Pt content in the Pt/C sample (% atomic) was 21.5 %. As in the last case, four peaks attributed to two spin-orbit coupling doublets were observed. Similar binding energies to the Pt/PANI/C sample were obtained. Pt^0 content in the Pt/C sample was 82.4 %. The peaks at 71.2 and 74.4 eV were attributed to metallic Pt [25-27]. The second doublet was located at 72.6 and 75.8 eV and was assigned to Pt^{2+} species [28, 29]. The content of Pt^{2+} species was 17.6 % of the total Pt content.

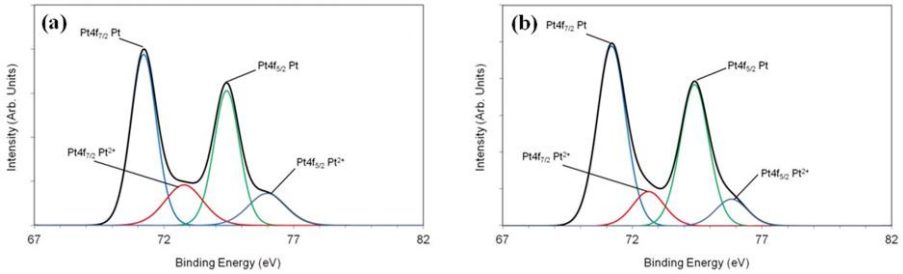

Figure 11. Pt4f XPS core level spectrum of: a) Pt/PANI/C specimen. b) Pt/C specimen.

Figure 12 shows the high resolution N1s spectrum for the PANI/C and PANI/Pt/C samples. Two binding energy peaks were recorded for the PANI/C sample in Figure 12a centred at 399.6 and 401.7 eV. The peak at 399.6 eV was assigned to the neutral amine-like (-NH-) structure which is characteristic of benzenoid rings [2, 30]. The other peak with binding energy > 400 eV was assigned to positively charged nitrogen atoms (N^+) [2, 30]. The doping ratio (N^+/N_{Total}) was 0.31; there is approximately one charged amine for three benzenoid rings.

Figure 12b shows the N1s XPS spectrum for the Pt/PANI/C sample. The signal obtained was deconvoluted into two contributions centered at 399.5 and 401.1 eV. The peak at 399.8 eV was assigned to neutral amine-like (-NH-) structure [2, 30]. The peak at 401.1 eV was ascribed to positively charged nitrogen atoms (N^+) [2, 30]. The doping ratio obtained was (N^+/N_{Total}) was 0.31. This value was the same obtained for PANI/C samples.

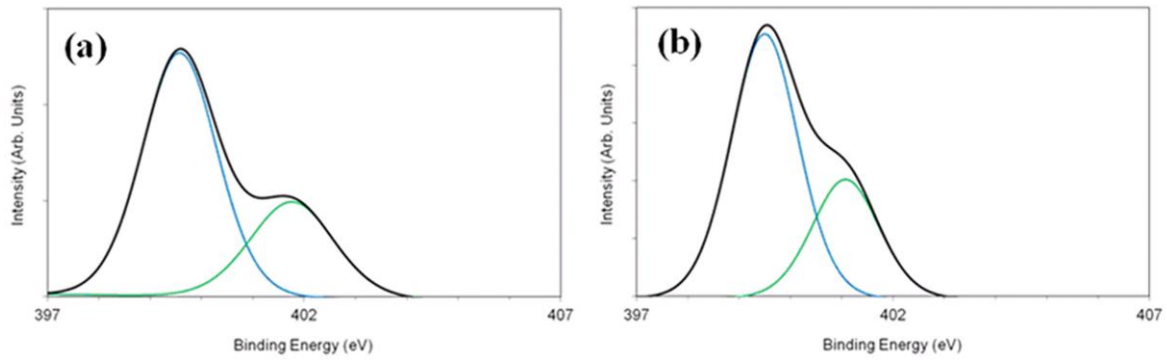

Figure 12. N1s XPS core level spectrum of: a) PANI/C specimen. b) Pt/PANI/C specimen.

4. CONCLUSIONS

In the present work a textile carbon fabric was successfully transformed into suitable working electrodes. Two types of modified electrodes: Pt/PANI/C and Pt/C were manufactured. The XPS analysis has shown that the platinum electrodeposited on Pt/C and Pt/PANI/C was mainly Pt^0. The doping ratio of the polymer in PANI/C and Pt/PANI/C was the same (N^+/N_{Total}) = 0.31. EIS analysis

indicates that Pt/PANI/C samples present the highest electroactivity. The conductivity, the counter-ions diffusion and the counter-ion exchange were increased significantly for Pt/PANI/C electrodes in comparison with the other materials. According with SEM results, a different distribution of the platinum particles was obtained. Pt/C electrode shows a compact distribution of platinum particles. On the other hand, the surface of Pt/PANI/C electrode shows a lower number of platinum particles and a more disperse distribution of the platinum. Modified electrodes were characterized in sulphuric and amaranth solutions by means of CV, LV, EIS and SECM techniques. Its electrochemical behavior was successfully contrasted with our own experimental information and information gathered from the literature. Thus, polarization curves of amaranth showed a characteristic peak at 460 mV for both Pt/PANI/C and Pt/C electrodes. This peak did not appear in the polarization curve for the bare carbon electrode. The characteristic peak of amaranth electrooxidation appeared when a starting potential of -200 mV was previously set. This last result allows to propose a treatment strategy based on the combined electroreduction/electrooxidation for the electrochemical treatment of azo dyes. Future investigation will be carried out with dimensionally larger CMEs developed from the results obtained in this work.

ACKNOWLEDGEMENTS

The authors would like to acknowledge to the Spanish Ministry of Science and Innovation (MICINN) for the financial support (CTM2010-18842-C02-02 and CTM 2011-23583), to the Universitat Politècnica de València (Vicerrectorado de Investigación PAID-06-10 contract 003-233) for the financial support and to the company Carbongen S.A., Cocentaina, Spain, that kindly donated the activated carbon fabric.

References

1. J. Molina, A. I. del Río, J. Bonastre, F. Cases, *Eur. Polym. J.*, 44 (2008) 2087.
2. J. Molina, M. F. Esteves, J. Fernández, J. Bonastre, F. Cases, *Eur. Polym. J.*, 47 (2011) 2003.
3. M. C. Venceslau, S. Tom, J. J. Simon, *Environ. Technol.*, 15 (1994) 917.
4. C. A. Martínez-Huitle, E. Brillas, *Appl. Catal. B.*, 87 (2009) 105.
5. M. Muthukumar, M. T. Karuppiah, G. B. Raju, *Sep. Purif. Technol.*, 55 (2007) 198.
6. N. Daneshvar, H. A. Sorkhabi, M. B. Kasiri, *J. Hazard. Mater.*, 112 (2004) 55.
7. O. T. Can, M. Bayramoglu, M. Kobya, *Ind. Eng. Chem. Res.* 42 (2003) 3391.
8. A. Fernandes, M. Morão, A. Magrinho, I. G. Lopes, *Dyes Pigments.*, 61 (2004) 287.
9. A. Faouzi, B. Nasr, G. Abdellatif, *Dyes Pigments*,73 (2007) 86.
10. J. Hastie, D. Bejan, M. T. León, N. J. Bunce, *Ind. Eng. Chem. Res.*, 46 (2006) 4898.
11. P. A. Carneiro, C. S. Fugivara, R. F. P. Nogueira, N. Boralle, M. V. B. Zanoni, *Port. Electrochim. Acta*, 2 2003 49.
12. M. C. Gutierrez, M. Pepió, M. Crespi, *Color. Technol.*, 118 (2002) 1.
13. M. Panizza, C. Bocca, G. Cerisola, *Water Res.*, 34 (2000) 2601.
14. A. I. Del Río, J. Fernández, J. Molina, J. Bonastre, *Electrochim. Acta*, 55 (2010) 7282.
15. L. Fan, Y. Zhou, W. Yang, G. Chen, F. Yang, *J. Hazard. Mater.*, B137 (2006) 1182.
16. W. U. Kezhong, M. Xu, W. Xindong, L. Jingling, *Rare Metals*, 24 (2005) 33.
17. L. M. Huang, W. R. Tang, T. Ch. Wen, *Journal of Power Sources*, 164 (2007) 519.
18. L. Niu, Q. Li, F. Wei, S. Wu, P. Liu, X. Cao, *J. Electroanal. Chem.*, 578 (2005) 331.
19. R. N. Singh, R. Awasthi, S. K. Tiwari, *Open Catal. J.*, 3 (2010) 50.

20. J. Molina, J. Fernández, A. I. del Río, J. Bonastre, F. Cases, *Applied Surface Science*, 258 (2012) 6246.
21. M. M. Khandpekar, R. K. Kushwaha, S. P. Pati, *Solid-State Electronics*, 62 (2011) 156.
22. P. Sun, F. O. Laforge, M. V. Mirkin, *Phys. Chem. Chem. Phys.* 9 (2007) 802.
23. L. Rajendran, S. P. Ananthi, *J. Electroanal. Chem.* 561 (2004) 113.
24. C. D. Wagner, A. V. Naumkin A. Kraut-Vass, J. W. Allison, C. J. Powell, J. R. Rumble, X-ray Photoelectron Spectroscopy Database, The National Institute of Standards.
25. W. Chen, S. Chen, *J. Mater. Chem.* 21 (2011) 9169.
26. R. Benoit, Y. Durand, B. Narjoux, G. Quintana, Y. Georges, X-Ray Photoelectron Spectroscopy Database. La Surface, CNRS and Thermo Fisher Scientific, Thermo Electron France. Available from: http://www.lasurface.com/database/elementxps.php
27. N. H. H. Abu Bakar, M. M. Bettahar, M. Abu Bakar, M. S. Monteverdi, J. Ismail, M. Alnot, *J. Catal.* 265 (2009) 63.
28. A. Drelinkiewicz, A. Zięba, J. Sobczak, M. Bonarowska, Z. Karpiński, A. Waksmundzka-Góra, J. Stejskal, *Reactive & Functional Polymers*, 69 (2009) 630.
29. S. Hu, J. Hou, L. Xiong, K. Weng, T. Yang, Y. Luo, *Sep. Purif. Technol.*, 77 (2011) 214.
30. E. T. Kang, K. G. Neoh, K. L. Tan, *Prog. Polym. Sci.* 23 (1998) 277.